Supporting Information for "Regional scale trends in column CO dominate over most urban scale trends over 16 years"

Jacob K. Hedelius[1,a], Geoffrey C. Toon[2,3], Rebecca R. Buchholz[4], Laura T. Iraci[5], James R. Podolske[5], Coleen M. Roehl[3], Paul O. Wennberg[3,6], Helen M. Worden[4], and Debra Wunch[1]

[1]Department of Physics, University of Toronto, Toronto, Ontario, Canada

[2]Jet Propulsion Laboratory, California Institute of Technology, Pasadena, California, USA

[3]Division of Geological and Planetary Sciences, California Institute of Technology, Pasadena, CA, USA

[4]Atmospheric Chemistry Observations and Modeling, National Center for Atmospheric Research, Boulder, Colorado, USA

[5]NASA Ames Research Center, Mountain View, CA, USA

[6]Division of Engineering and Applied Science, California Institute of Technology, Pasadena, California, USA

[a]Now at Space Dynamics Laboratory, Utah State University, North Logan, Utah, USA

Contents of this file

Corresponding author: Jacob K. Hedelius, Department of Physics, University of Toronto, Toronto, ON M5S 1A7, CAN. (jacob.hedelius@utoronto.ca)

4. Urban versus rural trends for additional cities

Introduction

Map of TransCom regions. Figure S1 is a map of the 23 TransCom regions. There are eleven predominantly land regions, and eleven predominantly water regions. Antarctica and Greenland are not optimized. A map with full names is in Gurney et al. (2003).

Figures of X_{CO} trends for additional case study urban areas.

Plots of X_{CO} behavior for additional cities are included in this section. These plots are included to aid in distinguishing behavior within a given urban area from a larger region. These are similar to Fig. 10 in the main text. Populations listed here are from the Global Human Settlement Urban Centre Database. For convenience we have copied a modified version of the caption here: Trends of MOPITT X_{CO} over a given urban area. (a) Colored points represent monthly averages of grid cells within the urban area as noted in (d). Gray heatmap is for monthly averages from all grid cells in full region. (b) Solid lines are averages of urban and non-urban grid cells. Red fill indicates higher urban X_{CO}, and blue fill indicates higher surrounding region X_{CO}. Percentiles of urban grids compared with those throughout the full region are shown as dots. (c) Gridded monthly differences correspond to the difference between solid lines in (b). Area monthly averages are averages within shown urban boundaries compared to the average outside of urban boundaries, but within 250 km of the center. Annual averages also shown. (d) Median X_{CO} values of the monthly averages. Red star marks the urban center. Purple triangles mark grid cells that define the urban area (which may be partially obstructed by the red star). Gray line indicates the urban boundaries. Cyan dots mark other urban areas with a population of at least 50,000. A Lambert azimuthal equal area projection

is used. (e) Same as (d), but showing the linear trend within each grid cell from fitting monthly averages from 2002–2017. (f) Map of population density, gridded to $0.1^\circ \times 0.1^\circ$.

References

Gurney, K. R., Law, R. M., Denning, A. S., Rayner, P. J., Baker, D., Bousquet, P., ... Yuen, C.-W. (2003, 4). TransCom 3 CO2 inversion intercomparison: 1. Annual mean control results and sensitivity to transport and prior flux information. *Tellus B*, *55*(2), 555–579. Retrieved from `http://www.tellusb.net/index.php/tellusb/article/view/16728` doi: 10.1034/j.1600-0889.2003.00049.x

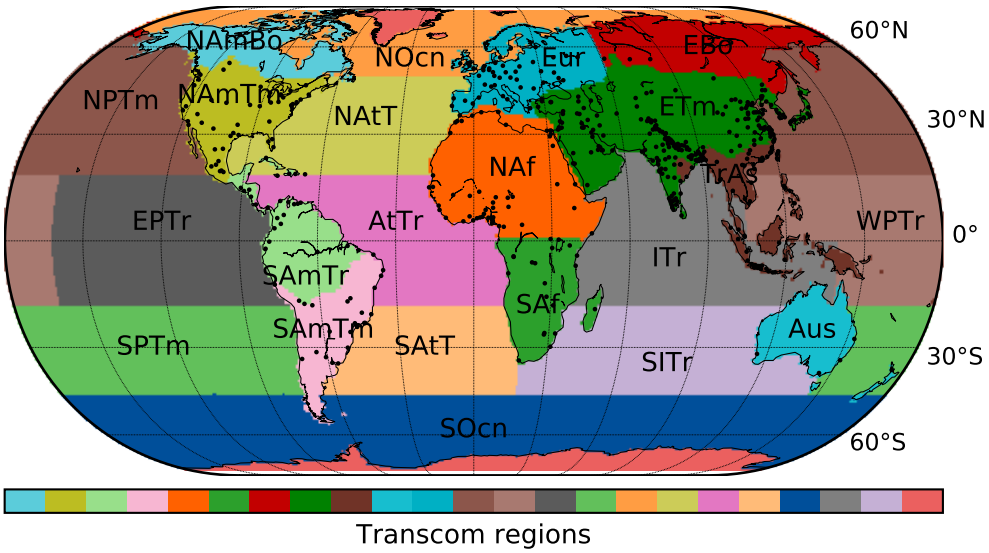

Figure S1. Map showing the different TransCom regions, labeled with their abbreviations. The 500 most populated cities are shown as black dots.

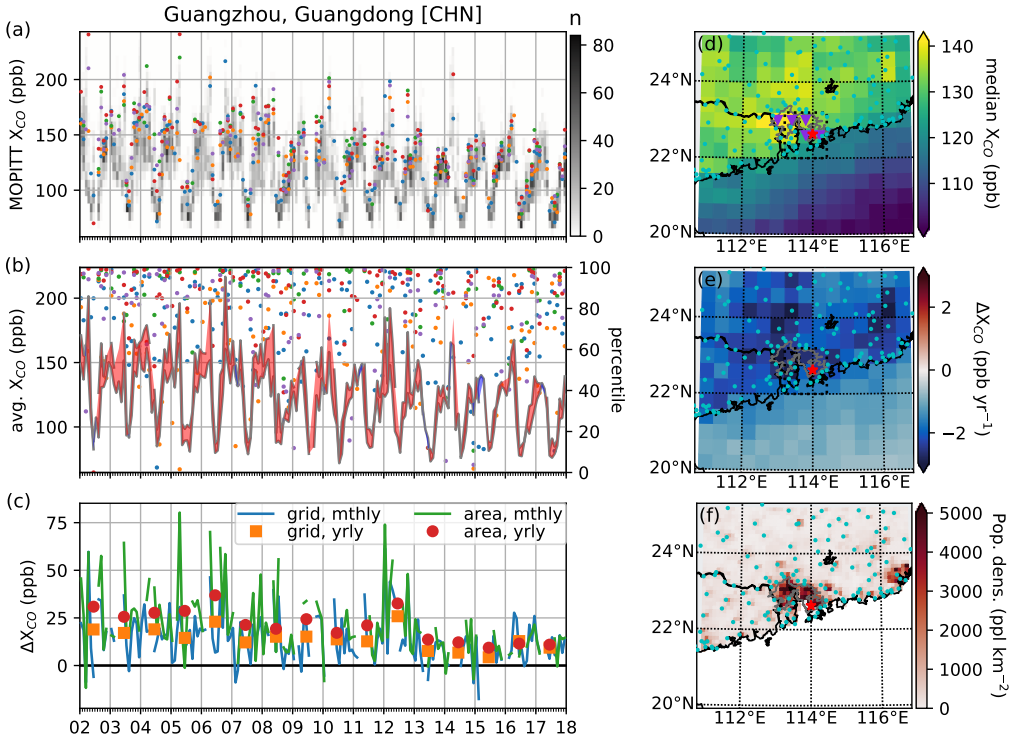

Figure S2. Guangzhou, China. Population: 40.6 million.

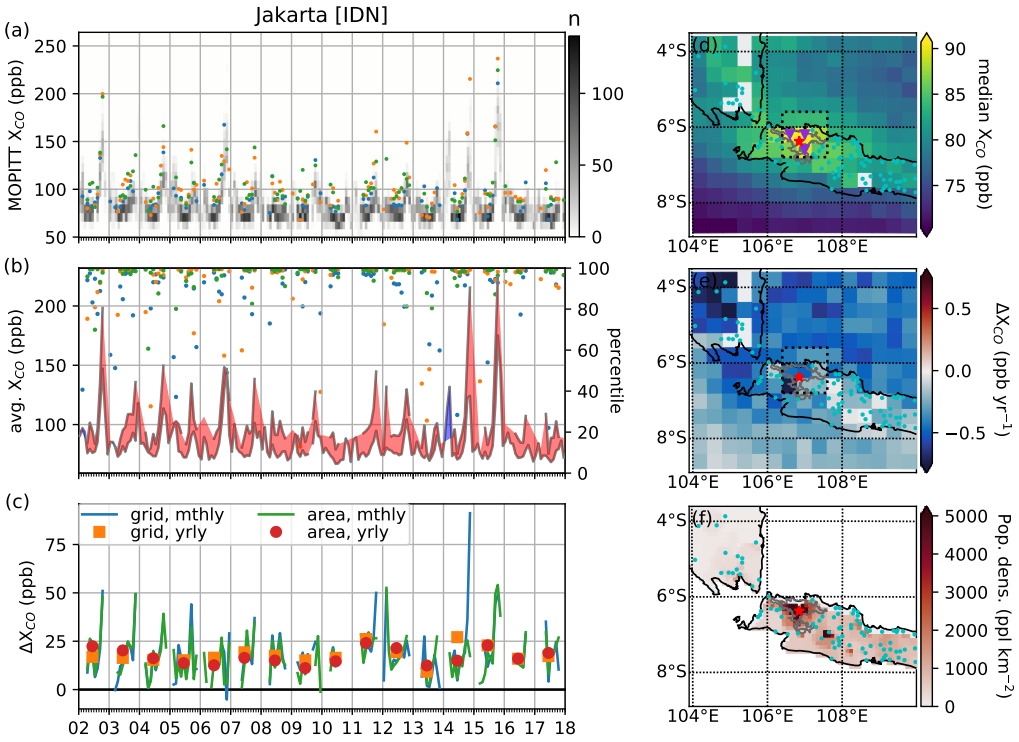

Figure S3. Jakarta, Indonesia. Population: 36.3 million.

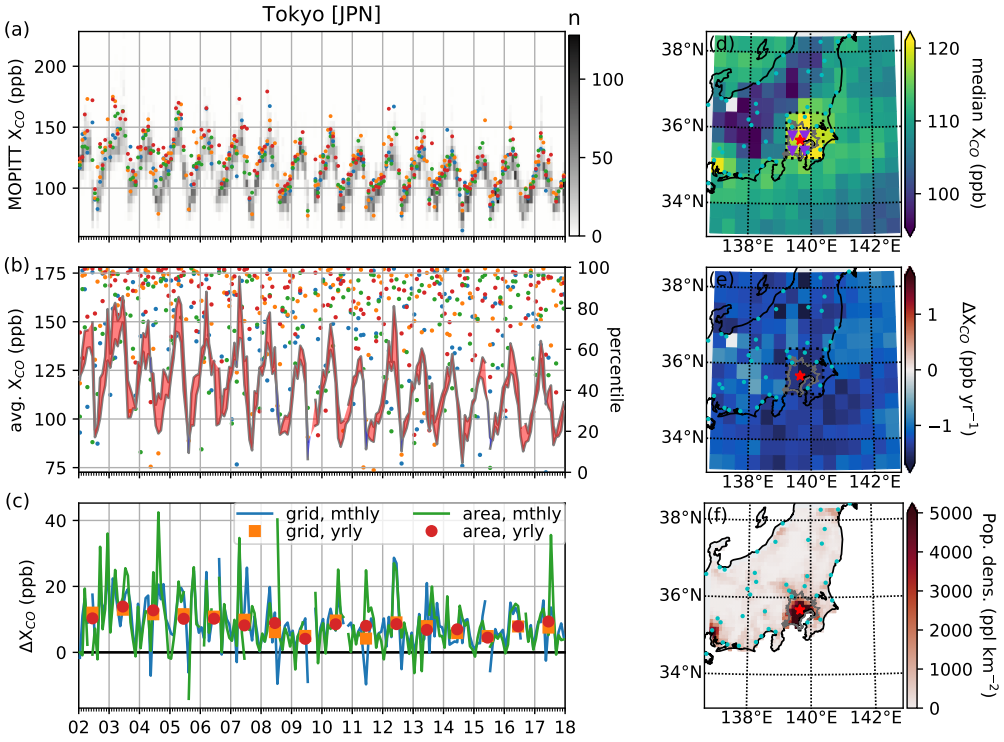

Figure S4. Tokyo, Japan. Population: 33.0 million.

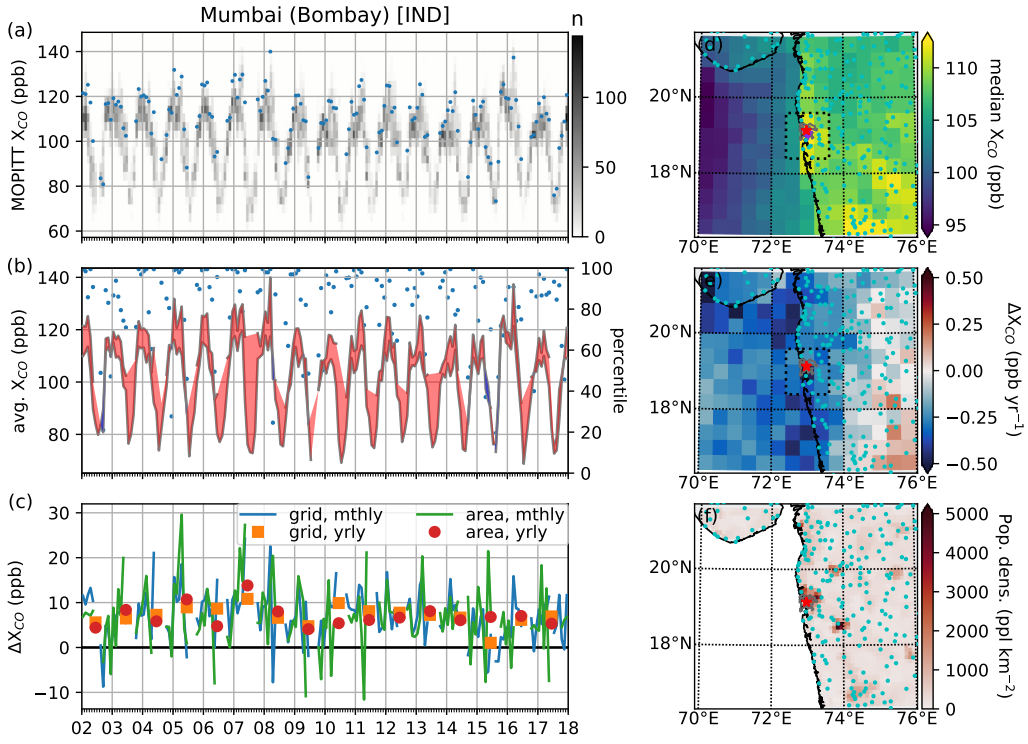

Figure S5. Mumbai, India. Population: 21.8 million.

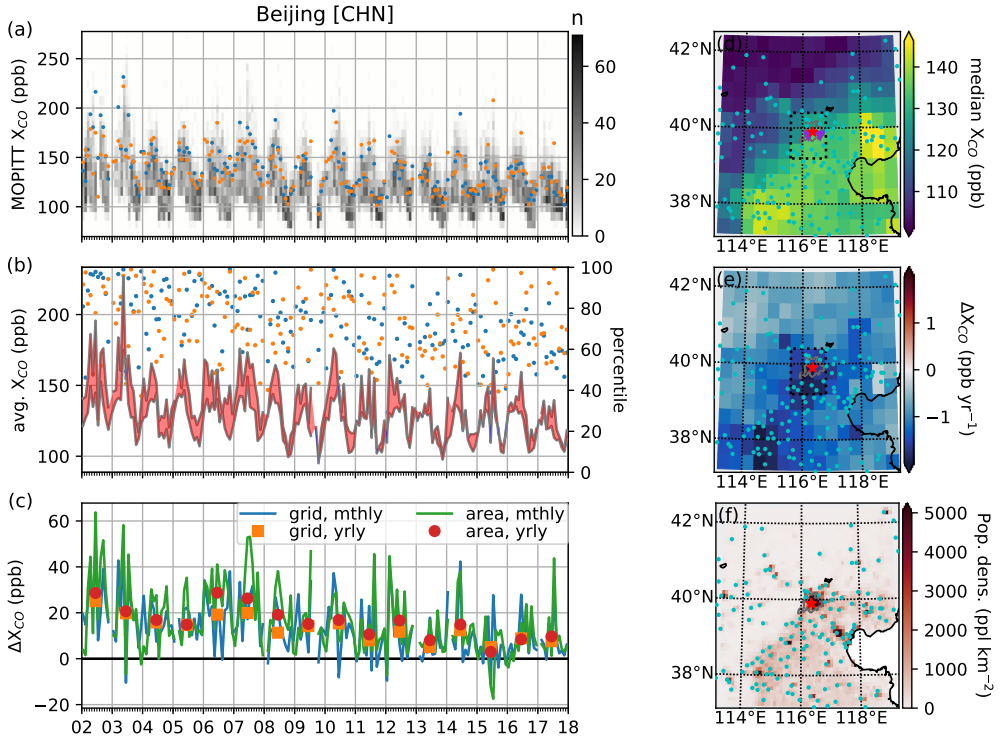

Figure S6. Beijing, China. Population: 18.0 million.

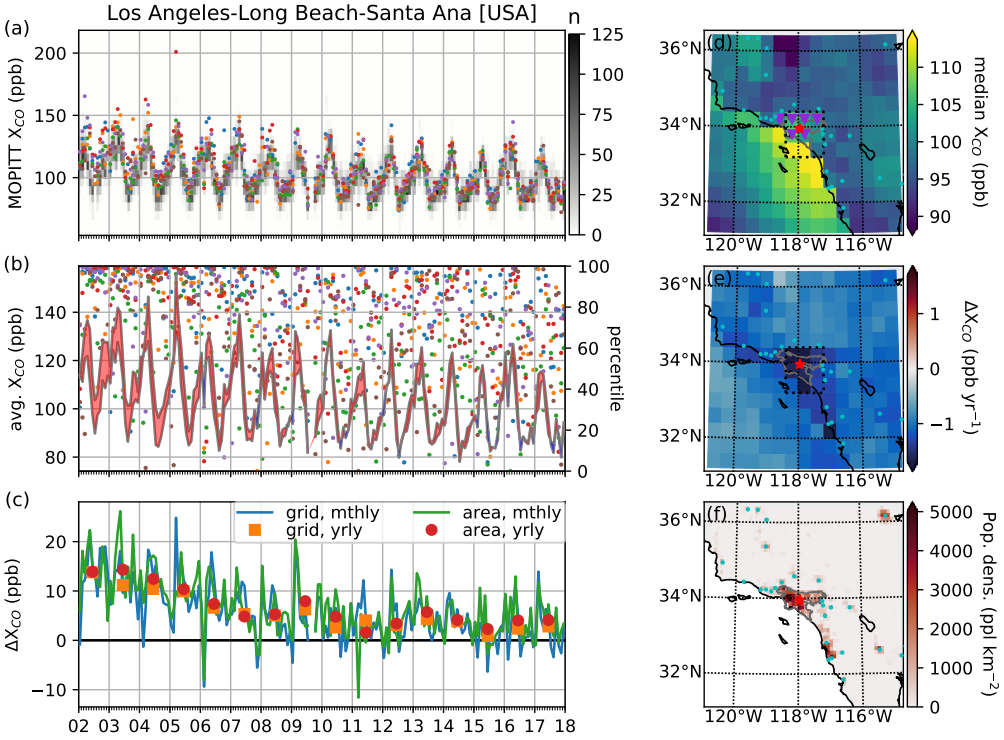

Figure S7. Los Angeles, United States. Population: 14.3 million.

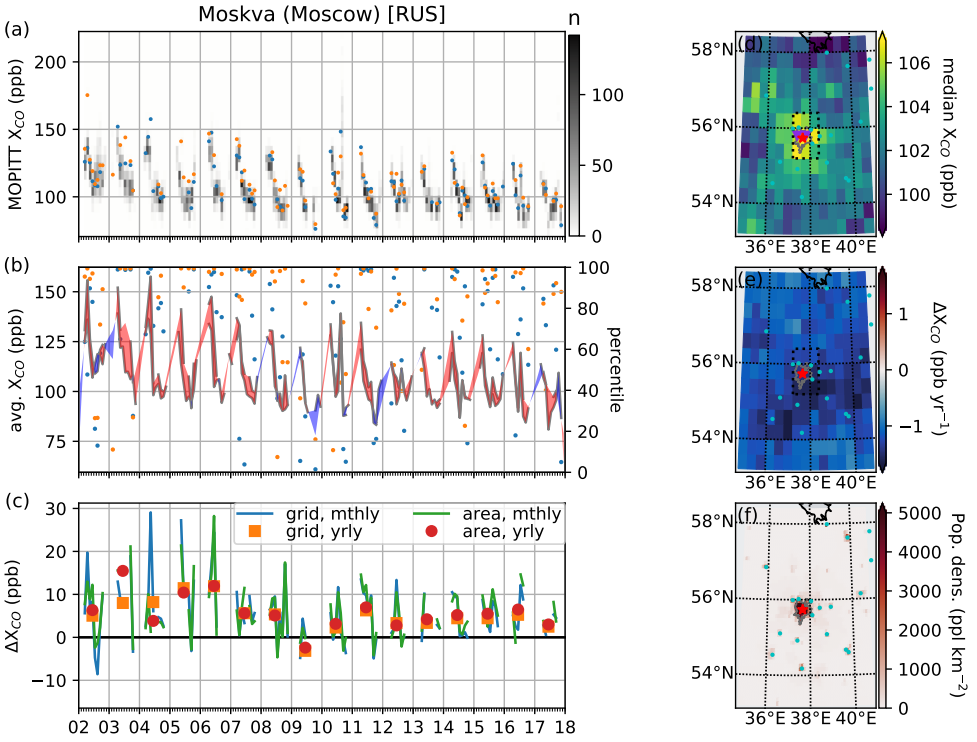

Figure S8. Moscow, Russia. Population: 14.1 million.

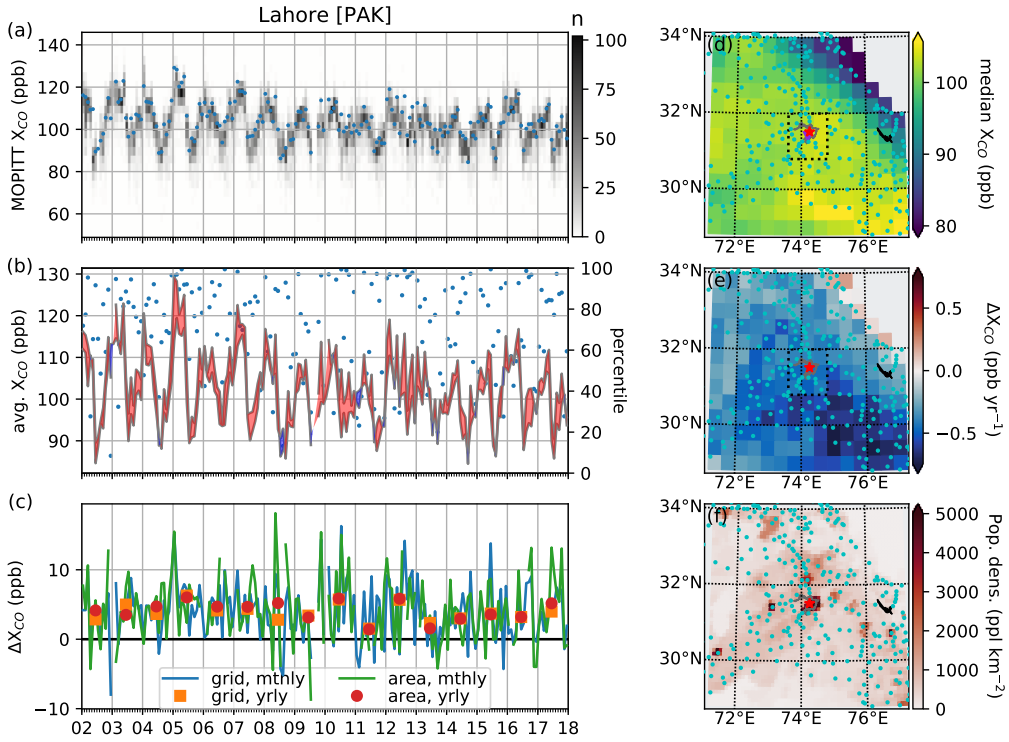

Figure S9. Lahore, Pakistan. Population: 10.1 million.

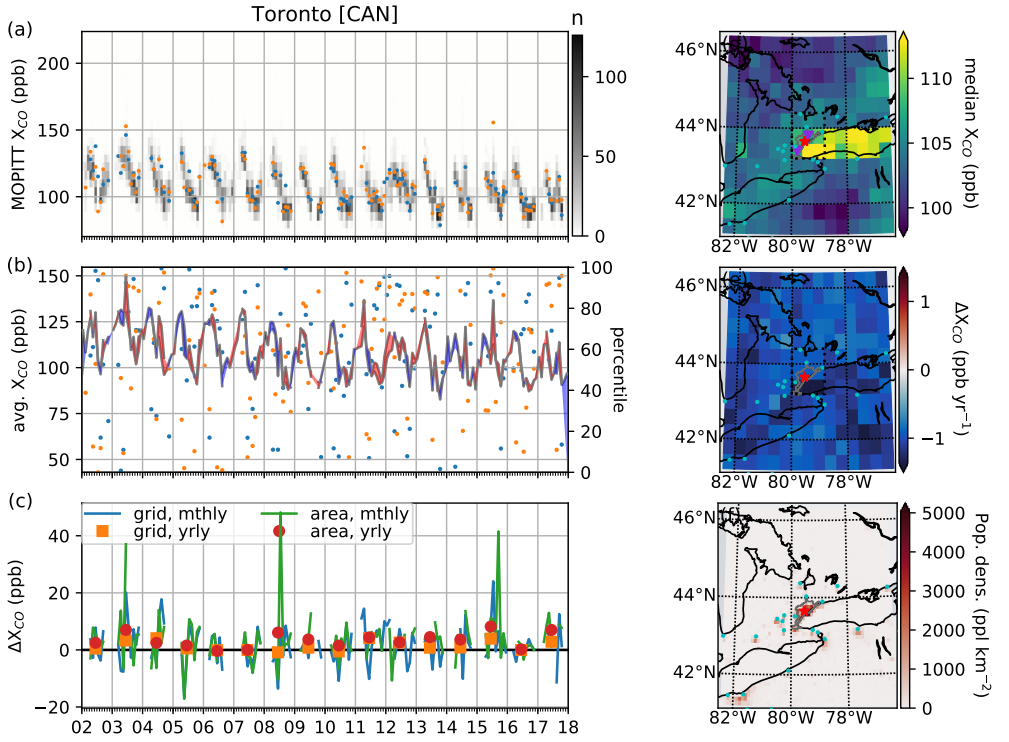

Figure S10. Toronto, Canada. Population: 6.0 million.

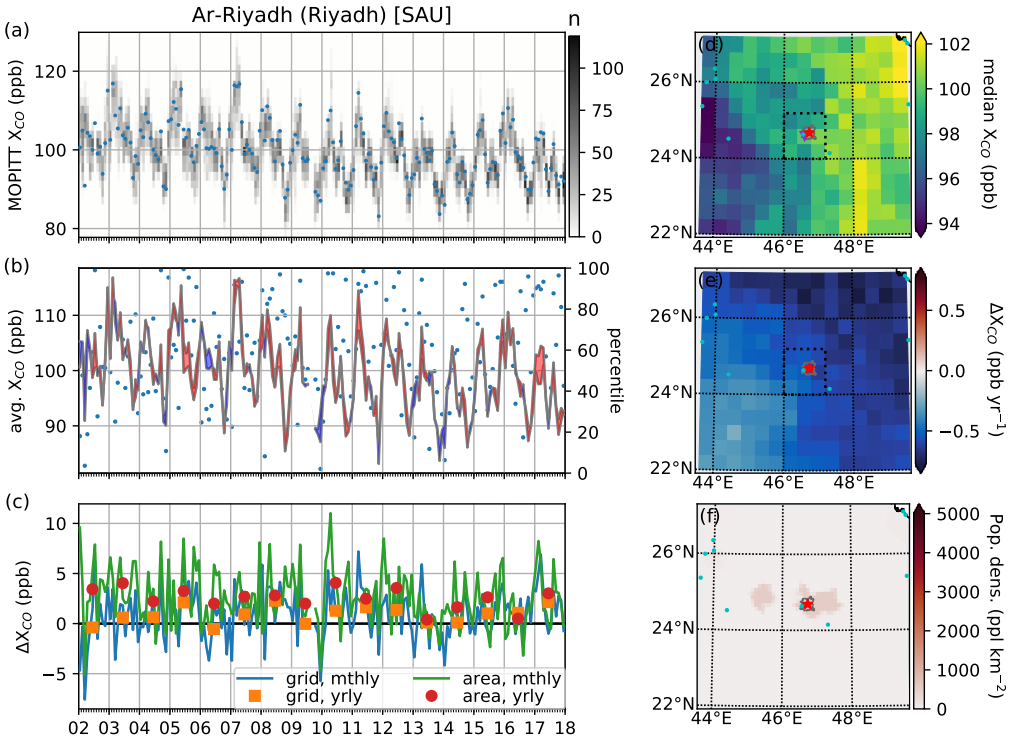

Figure S11. Riyadh, Saudi Arabia. Population: 5.7 million.

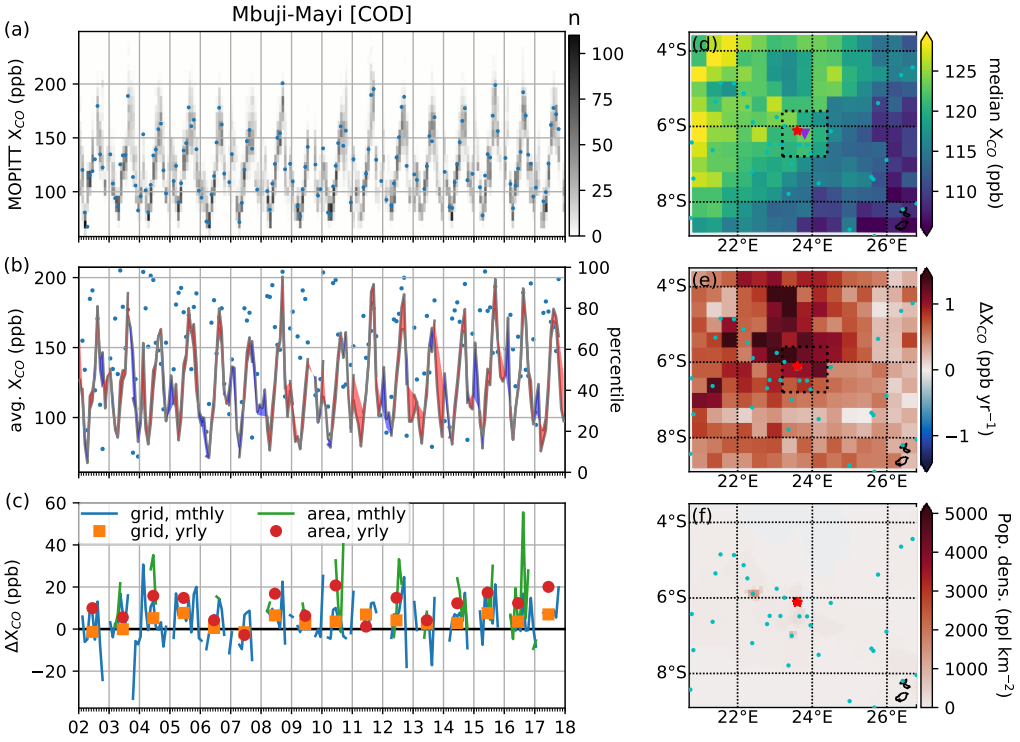

Figure S12. Mbuji-Mayi, Democratic Republic of the Congo. Population: 3.0 million.

Urban trends compared with regions These plots show the trend differences between the urban areas and the surrounding region (within 250 km). Error bars represent the 95 % confidence interval. Along the y-axis are the names for the largest cities within the urban area, along with the population. Figures S13–S16. Usually the trend in the urban area is not significantly different from that of the surrounding region. For these cities the median difference is $-0.04\,\mathrm{ppb\,yr^{-1}}$ and the average is $-0.09 \pm 0.77(1\sigma)\,\mathrm{ppb\,yr^{-1}}$.

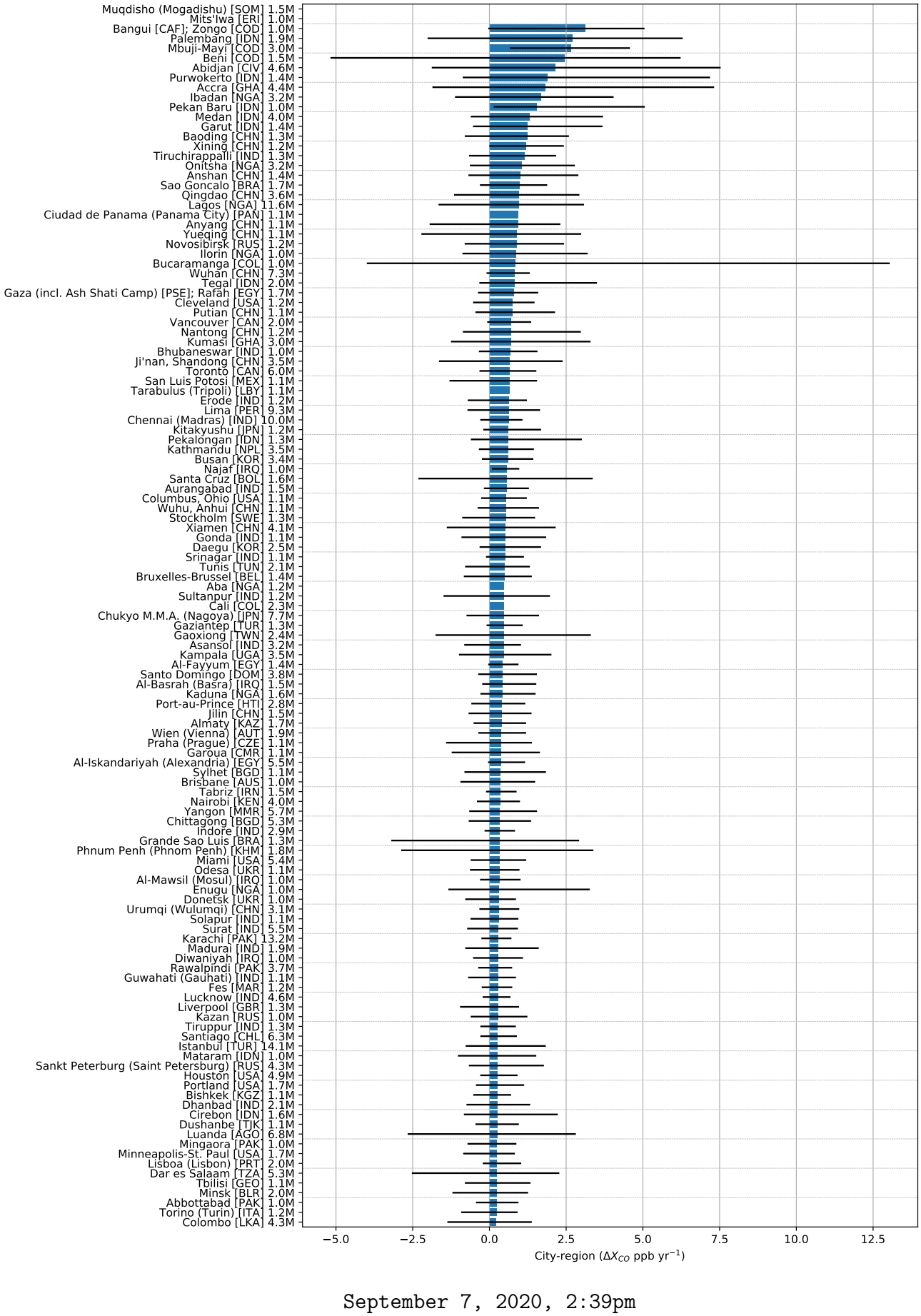

Figure S13. Trend differences for urban areas 1–125.

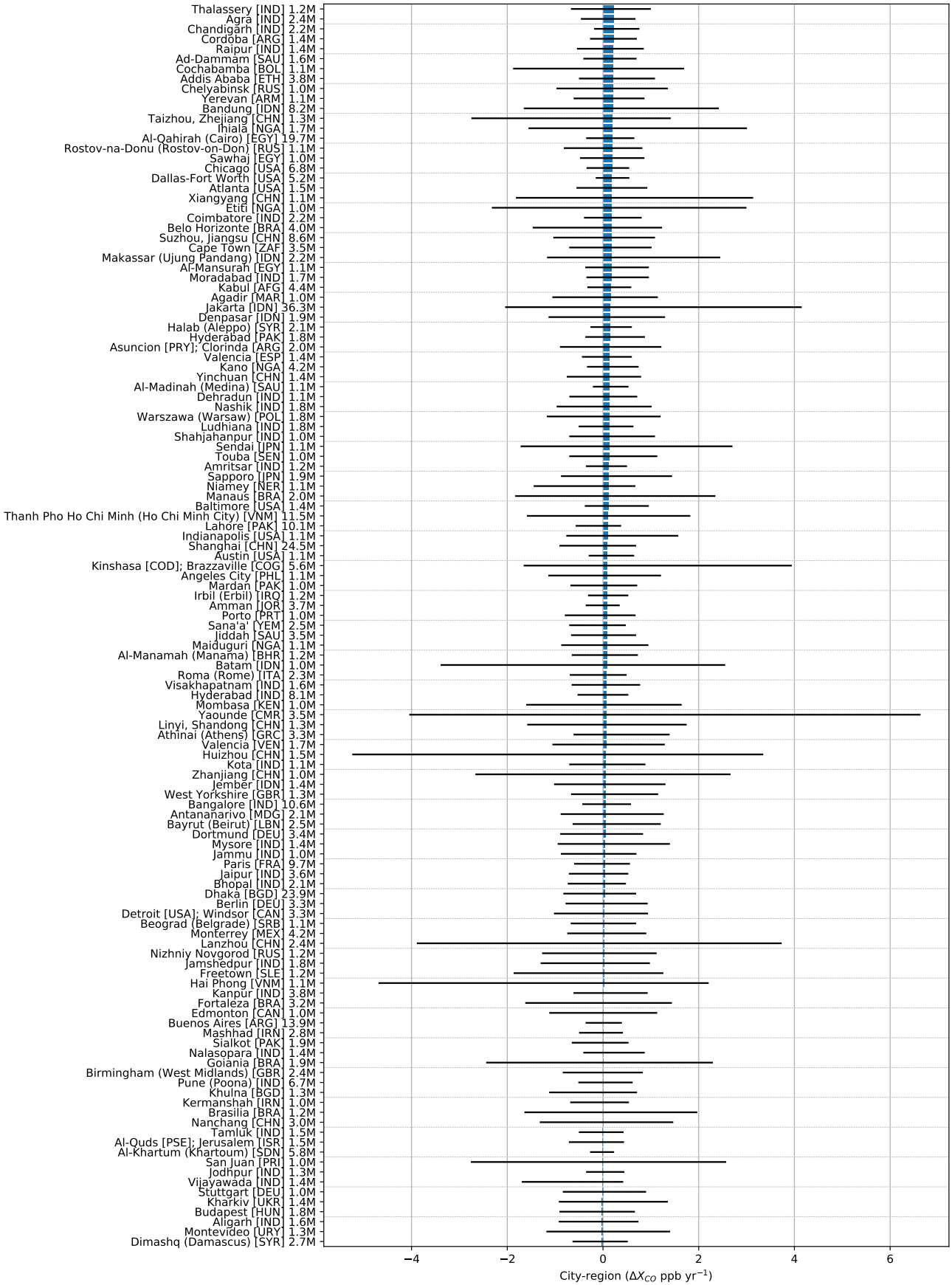

September 7, 2020, 2:39pm

Figure S14. Trend differences for urban areas 126–250.

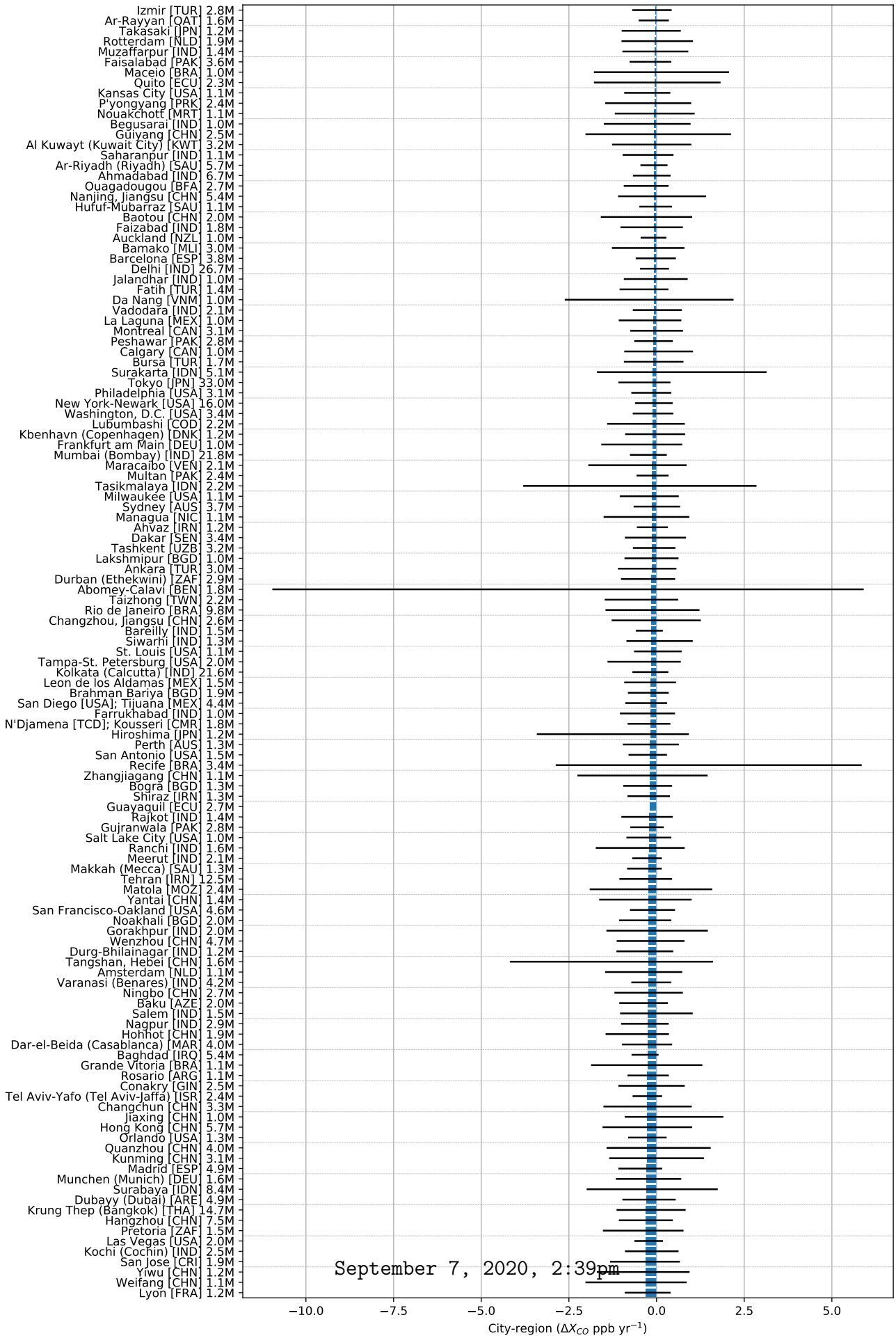
Izmir [TUR] 2.8M
Ar-Rayyan [QAT] 1.6M
Takasaki [JPN] 1.2M
Rotterdam [NLD] 1.9M
Muzaffarpur [IND] 1.4M
Faisalabad [PAK] 3.6M
Maceio [BRA] 1.0M
Quito [ECU] 2.3M
Kansas City [USA] 1.1M
P'yongyang [PRK] 2.4M
Nouakchott [MRT] 1.1M
Begusarai [IND] 1.0M
Guiyang [CHN] 2.5M
Al Kuwayt (Kuwait City) [KWT] 3.2M
Saharanpur [IND] 1.1M
Ar-Riyadh (Riyadh) [SAU] 5.7M
Ahmadabad [IND] 6.7M
Ouagadougou [BFA] 2.7M
Nanjing, Jiangsu [CHN] 5.4M
Hufuf-Mubarraz [SAU] 1.1M
Baotou [CHN] 2.0M
Faizabad [IND] 1.8M
Auckland [NZL] 1.0M
Bamako [MLI] 3.0M
Barcelona [ESP] 3.8M
Delhi [IND] 26.7M
Jalandhar [IND] 1.0M
Fatih [TUR] 1.4M
Da Nang [VNM] 1.0M
Vadodara [IND] 2.1M
La Laguna [MEX] 1.0M
Montreal [CAN] 3.1M
Peshawar [PAK] 2.8M
Calgary [CAN] 1.0M
Bursa [TUR] 1.7M
Surakarta [IDN] 5.1M
Tokyo [JPN] 33.0M
Philadelphia [USA] 3.1M
New York-Newark [USA] 16.0M
Washington, D.C. [USA] 3.4M
Lubumbashi [COD] 2.2M
Kbenhavn (Copenhagen) [DNK] 1.2M
Frankfurt am Main [DEU] 1.0M
Mumbai (Bombay) [IND] 21.8M
Maracaibo [VEN] 2.1M
Multan [PAK] 2.4M
Tasikmalaya [IDN] 2.2M
Milwaukee [USA] 1.1M
Sydney [AUS] 3.7M
Managua [NIC] 1.1M
Ahvaz [IRN] 1.2M
Dakar [SEN] 3.4M
Tashkent [UZB] 3.2M
Lakshmipur [BGD] 1.0M
Ankara [TUR] 3.0M
Durban (Ethekwini) [ZAF] 2.9M
Abomey-Calavi [BEN] 1.8M
Taizhong [TWN] 2.2M
Rio de Janeiro [BRA] 9.8M
Changzhou, Jiangsu [CHN] 2.6M
Bareilly [IND] 1.5M
Siwarhi [IND] 1.3M
St. Louis [USA] 1.1M
Tampa-St. Petersburg [USA] 2.0M
Kolkata (Calcutta) [IND] 21.6M
Leon de los Aldamas [MEX] 1.5M
Brahman Bariya [BGD] 1.9M
San Diego [USA]; Tijuana [MEX] 4.4M
Farrukhabad [IND] 1.0M
N'Djamena [TCD]; Kousseri [CMR] 1.8M
Hiroshima [JPN] 1.2M
Perth [AUS] 1.3M
San Antonio [USA] 1.5M
Recife [BRA] 3.4M
Zhangjiagang [CHN] 1.1M
Bogra [BGD] 1.3M
Shiraz [IRN] 1.3M
Guayaquil [ECU] 2.7M
Rajkot [IND] 1.4M
Gujranwala [PAK] 2.8M
Salt Lake City [USA] 1.0M
Ranchi [IND] 1.6M
Meerut [IND] 2.1M
Makkah (Mecca) [SAU] 1.3M
Tehran [IRN] 12.5M
Matola [MOZ] 2.4M
Yantai [CHN] 1.4M
San Francisco-Oakland [USA] 4.6M
Noakhali [BGD] 2.0M
Gorakhpur [IND] 2.0M
Wenzhou [CHN] 4.7M
Durg-Bhilainagar [IND] 1.2M
Tangshan, Hebei [CHN] 1.6M
Amsterdam [NLD] 1.1M
Varanasi (Benares) [IND] 4.2M
Ningbo [CHN] 2.7M
Baku [AZE] 2.0M
Salem [IND] 1.5M
Nagpur [IND] 2.9M
Hohhot [CHN] 1.9M
Dar-el-Beida (Casablanca) [MAR] 4.0M
Baghdad [IRQ] 5.4M
Grande Vitoria [BRA] 1.1M
Rosario [ARG] 1.1M
Conakry [GIN] 2.5M
Tel Aviv-Yafo (Tel Aviv-Jaffa) [ISR] 2.4M
Changchun [CHN] 3.3M
Jiaxing [CHN] 1.0M
Hong Kong [CHN] 5.7M
Orlando [USA] 1.3M
Quanzhou [CHN] 4.0M
Kunming [CHN] 3.1M
Madrid [ESP] 4.9M
Munchen (Munich) [DEU] 1.6M
Surabaya [IDN] 8.4M
Dubayy (Dubai) [ARE] 4.9M
Krung Thep (Bangkok) [THA] 14.7M
Hangzhou [CHN] 7.5M
Pretoria [ZAF] 1.5M
Las Vegas [USA] 2.0M
Kochi (Cochin) [IND] 2.5M
San Jose [CRI] 1.9M
Yiwu [CHN] 1.2M
Weifang [CHN] 1.1M
Lyon [FRA] 1.2M
September 7, 2020, 2:39pm
−10.0
−7.5
−5.0
−2.5
0.0
2.5
5.0
City-region (ΔX_{CO} ppb yr^{-1})

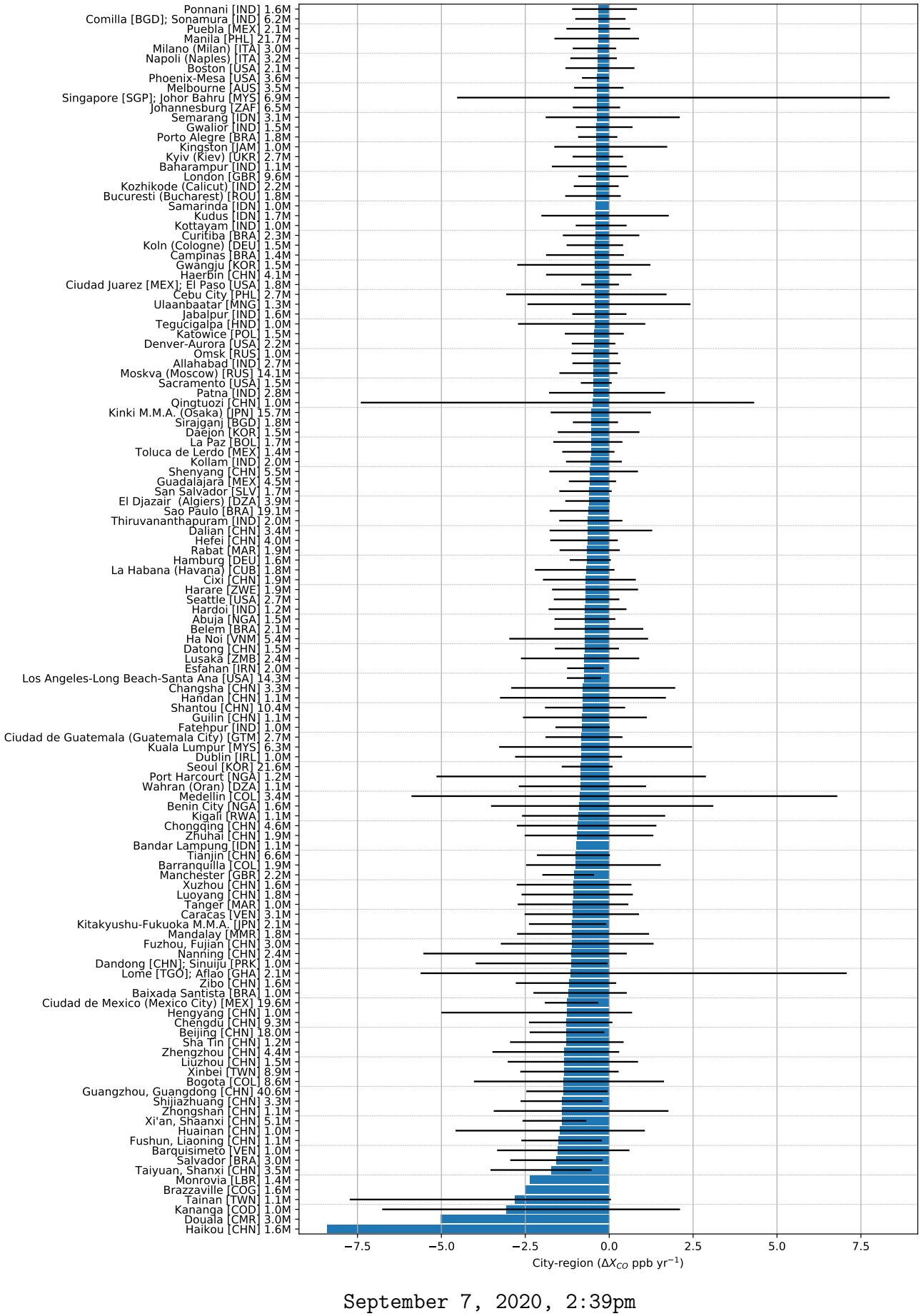

Figure S16. Trend differences for urban areas 376–500.